Frontiers in Built Environment
TYPE Methods
PUBLISHED 28 February 2025
DOI 10.3389/fbuil.2025.1542216

Check for updates

OPEN ACCESS

EDITED BY
Wei Guo,
Tianjin University, China

REVIEWED BY
Fayun Liang,
Tongji University, China
Hongtao Fu,
Wenzhou University, China

*CORRESPONDENCE
Sijie Liu,
sijieliu@whu.edu.cn

RECEIVED 09 December 2024
ACCEPTED 10 February 2025
PUBLISHED 28 February 2025

CITATION
Han C, Fan Z, Liu S, Bai X, Yu P, Wu W, Mao X, Liu Y, Liu Z and Bai B (2025) Double drainage consolidation of annular soil pile considering radial deformation.
Front. Built Environ. 11:1542216.
doi: 10.3389/fbuil.2025.1542216

Double drainage consolidation of annular soil pile considering radial deformation

Chao Han[1], Zhou Fan[1], Sijie Liu[2]*, Xinyue Bai[2], Peng Yu[1], Wei Wu[1], Xintong Mao[1], Yunfei Liu[1], Zhiwei Liu[1] and Bin Bai[1]

[1]State Grid Jiangsu Electric Power Co., Ltd. Construction Company, Nanjing, China, [2]School of Civil Engineering, Wuhan University, Wuhan, China

The resource utilization of silt with high water content is a major problem in the process of ecological dredging and engineering construction in recent years. It is a feasible way to realize the resource utilization of silt into hollow pile section by means of central pressure. The preparation of central pressurized annular soil pile is mainly based on the principle of soil drainage and consolidation, but the deformation direction and external force loading mode are different from the classical consolidation theory. Based on the connotation of this technique, the calculation model considering radial deformation is derived. Combining the control equation and solution conditions, the finite element solution of soil pile with the radial deformation is obtained. Based on this solution, the influence of the related factors in the preparation process of annular soil pile, including the initial water content, external load size, internal and external diameter size and nonlinear compression index, on the development of consolidation degree and the growth of internal diameter in the preparation process is studied.

KEYWORDS

consolidation, soft soil, circular soil pile, radial deformation, non-linear

1 Introduction

With the vigorous promotion of the strategy of transportation power and the construction of ecological civilization, the problem of waste mud disposal generated in the process of water ecological environment management and engineering construction has become increasingly prominent (Zhang et al., 2014; Zhu et al., 2012). Drainage and consolidation method is a common soft soil reinforcement method (Nguyen et al., 2020). Common drainage consolidation method, such as: stacking preloading method (Chu et al., 2006), vacuum prepressing method (Indraratna et al., 2005), through the soil along the vertical into the drainage plate, at

Abbreviations: H, Length of prepared soil pile(m); r, Epansion direction of soil pile; z, Length direction of hollow soil pile(m); $r_{n,}$ Hollow inner radius before extrusion begins(m); $r_{w.}$ Outer radius of prepared soil pile(m); r_f, Internal radius of extrusion molding(m); σ_r, Stress in expansion direction of soil pile (kPa); e, Porosity ratio; σ', Effective stress (kPa); dV, Deformation of the element; dq_r, Radial seepage increment; u, Pore pressure (kPa); $K_{r,}$ Nonlinear variation of the permeability coefficient; p, External pressure (kPa); U_P, Average pore water pressure consolidation degree; w, Initial water content (%); C_c, Compression index; σ_0', Initial effective stress; γ_w, Unit weight of water; σ_{r_n}, Stress at the radius of r_n; v_r^w, Velocity of radial drainage; $d\theta$, Angle of the unit; dz, Thickness of the unit; dr, Length of the unit in radial direction; k_{r0}, Permeability coefficient in the radial direction.

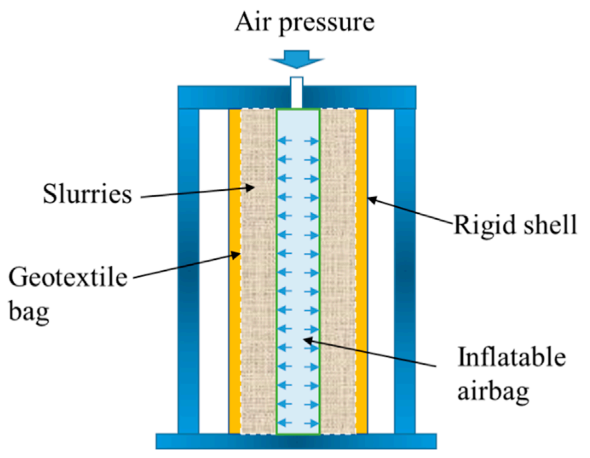

FIGURE 1
Construction method of annular soil piles.

the same time above the stacking load pressure or vacuum negative pressure, form a pressure difference in the soil and discharge the water in the soil. The stacking preloading method and vacuum prepressing method are often applicable to the local reinforcement treatment of large area silt site, and the cost is relatively low.

In addition to the two *in situ* treatment methods mentioned above, reinforcing sludge to use as backfill or foundation reinforcement components is also an efficient treatment approach. For instance, using mechanical dewatering methods combined with flocculation and solidification principles to prepare high-quality backfill materials (Han et al., 2023). Besides, after squeezing the sludge, it can be directly formed into foundation treatment components, which can greatly improve the utilization efficiency of the sludge. Preparing hollow soil piles from high water content slurry, Zhang (Zhang et al., 2022) proposed a ring-shaped soil pile preparation technology that involves applying pressure in a circumferential direction to dehydrate the surrounding fixed boundary soil. In this technology, the external load is achieved by inflating a bag placed in the center of the cylinder with water or gas under a certain pressure as shown in Figure 1.

For conventional surcharge or vacuum preloading drainage consolidation methods, the corresponding consolidation calculation theories have undergone a considerable period of development. In general, for soft ground surcharge preloading and vacuum preloading calculations, the computational area is equated to a cylindrical body surrounding the drainage plate or sand well to establish the corresponding consolidation model, and analytical or numerical methods are used for the solution (Geng et al., 2012). From the initial ideal sand well solutions, consolidation models have gradually developed that can consider nonlinear compressibility and permeability (Lekha et al., 1998), consolidation models that can consider well resistance effects (Deng et al., 2013), and consolidation models for high water content mud that consider clogging effects (Liu et al., 2021). In recent years, the computational models for consolidation problems have become increasingly close to actual conditions, such as using the equivalent method of annular drainage plates instead of the previously used area and perimeter equivalent methods (Lu et al., 2022), and using continuous boundary conditions to consider the actual drainage capacity of the interface, replacing the consolidation calculation models that previously assumed completely permeable or completely impermeable boundary conditions (Zong et al., 2019).

It is noteworthy that in the aforementioned model, the direction of deformation is assumed to be vertical, which means settlement occurs (Indraratna et al., 2005). External loads and surcharge are considered in the same direction as the deformation or in the form of negative pressure boundary conditions. However, during the preparation of prefabricated annular soil pile foundations using the drainage consolidation method, the external force is the central thrust of the soil pile, applied radially to the soil, and the deformation of the soil is mainly the change in radius. Therefore, the aforementioned existing models cannot accurately describe the drainage consolidation process of preparing annular soil piles.

In response to the lack of consolidation theory in the current preparation process of annular soil piles, this paper establishes a consolidation calculation model for annular soil piles considering central radial pressure based on the preparation principle of annular soil piles. It fully considers the nonlinearity of soil compression and permeability to establish the corresponding consolidation control equations, and uses the finite element method for precise solutions. Based on this model, a series of computational analyses have been carried out on the influence of related parameters, including initial radius, load size, and nonlinearity ratio.

2 Introduction of the preparation technology of ring soil pile

The preparation process of high water content mud is divided into the following steps. First place the prepaid gas or liquid loading pocket into the space in the ring pocket. Subsequently, the mud bag was filled with sufficient mud. After the mud is filled, fill the gas or liquid into the central loading sac, and control the pressure to the specified size. The inner diameter of the bag in the surrounding mud filling sac increases under the action of the central pressure. In order to ensure the stable shape of the soil pile, the outer wall of the mud-filling bag remains fixed. At the radius of the mud column in contact with the annular pocket, the external load is equal. In this technique, in order to make the water in the mud bag can be discharged quickly, the mud bag is wrapped in the geotextile, so the inner and outer walls of the soil pile can be regarded as permeable surface during the reinforcement Aprocess. The consolidation deformation of conventional soft land base mostly occurs in the vertical direction, but in the process of internal compression preparation of annular soil pile, the deformation occurs in the radial direction, consistent with the seepage direction, so it needs to be modeling and analyzed.

3 Establishment of the consolidation model

3.1 Model building

According to the technical points in Section 2, the actual compressed drainage consolidation of soil pile can be simplified to the consolidation model as shown in Figure 2, P represents the

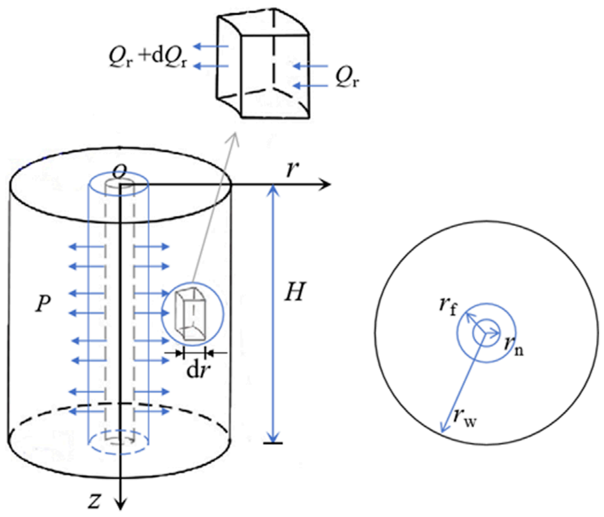

FIGURE 2
Schematic diagram of the consolidation model.

central plus load, H represents the length of prepared soil pile, r represents the expansion direction of soil pile, z is the length direction of hollow soil pile, r_n indicates the hollow inner radius before extrusion begins, r_w represents the outer radius of prepared soil pile, r_f represents the internal radius of extrusion molding.

3.2 Basic assumptions

The consolidation model has the following basic assumptions:

(1) The soil is saturated, and the soil particles and water are incompressible, and the soil deformation volume is equal to the discharge volume of pore water;
(2) Soil deformation only occurs in the radial direction, and no deformation occurs along the height direction of the soil pile;
(3) Soil seepage follows Darcy's law;
(4) The external load is applied from the inside of the annular soil pile and remains unchanged during the consolidation process;
(5) The radial strain is assumed to satisfy the small strain assumption.

3.3 Governing equation

3.3.1 Equilibrium equation

For a microelement, Equation 1 is held.

$$\sigma r \mathrm{d}z = (\sigma + \mathrm{d}\sigma)(r + \mathrm{d}r)\mathrm{d}z \tag{1}$$

Equation 2 could be derived that,

$$\frac{\partial \sigma(r,z,t)}{\partial r} = \frac{\sigma_r}{r} \tag{2}$$

3.3.2 Compressibility and permeability equations

The compressiblity can be expressed as Equation 3,

$$e = e_0 - C_c \log_{10}\left(\frac{\sigma'}{\sigma'_0}\right) \tag{3}$$

The permeability can be described by Darcy's law as Equations 4, 5,

$$i_r = \frac{1}{\gamma_w}\frac{\partial u}{\partial r} \tag{4}$$

$$v_r = v_r^w = -k_r i_r \tag{5}$$

3.3.3 Continuity equation

Assuming a microelement at the radial coordinate of x, according to the principle of continuous seepage deformation, the unit deformation is equal to its seepage increment as shown in Equation 6,

$$\mathrm{d}V = \mathrm{d}q_r \tag{6}$$

where $\mathrm{d}V$ represents the deformation of the element, $\mathrm{d}q_r$ represents the radial seepage increment. The radial seepage increment is in the Equations 7–9,

$$q_r = v_r^w r \mathrm{d}z \mathrm{d}\theta \tag{7}$$

$$q_r + \mathrm{d}q_r = \left\{v_r^w + \frac{\partial}{\partial r}[v_r^w]\mathrm{d}r\right\}(r + \mathrm{d}r)\mathrm{d}\theta \mathrm{d}z \tag{8}$$

$$\mathrm{d}q_r = v_r^w \mathrm{d}\theta \mathrm{d}r \mathrm{d}\xi + \frac{\partial}{\partial r}[v_r^w] r \mathrm{d}\theta \mathrm{d}r \mathrm{d}z \tag{9}$$

Replacing deformation into Equation 6, the continuity equation can be expressed as

$$\frac{v_r^w}{r} + \frac{\partial}{\partial r}(v_r^w) = -\frac{1}{1+e_0}\frac{\partial e}{\partial t} \tag{10}$$

According to the relationship between pore pressure and hydraulic gradient, it can be obtained that,

$$v_r^w = -\frac{k_r}{\gamma_w}\frac{\partial u}{\partial r} \tag{11}$$

Substituting Equation 11 into Equation 10, it can be derived as Equations 12, 13,

$$-\frac{k_r}{\gamma_w}\frac{1}{r}\frac{\partial u}{\partial r} + \frac{\partial}{\partial r}\left(-\frac{k_r}{\gamma_w}\frac{\partial u}{\partial r}\right) = -\frac{1}{1+e_0}\frac{\partial e}{\partial t} \tag{12}$$

That is,

$$\frac{1}{r\gamma_w}\frac{\partial}{\partial r}\left(r k_r \frac{\partial u}{\partial r}\right) = \frac{1}{1+e_0}\frac{\partial e}{\partial t} \tag{13}$$

The nonlinear variation of the permeability coefficient can be expressed as Equations 14, 15,

$$k_r = k_{r0} \times 10^{(e-e_0)/C_{kr}} \tag{14}$$

$$\frac{\partial \sigma'}{\partial r} = -\frac{\sigma'_0 \times \ln 10}{C_c} 10^{(e_0-e)/C_c} \frac{\partial e}{\partial r} \tag{15}$$

The equilibrium equation for combining the horizontal direction as Equation 16 shows,

$$-\frac{\sigma_r}{r} = -\frac{\sigma_0' \times \ln 10}{C_c} 10^{(e_0-e)/C_c} \frac{\partial e}{\partial r} + \frac{\partial u}{\partial r} \tag{16}$$

When the external pressure p is applied in the middle, the stress can be expressed as Equation 17,

$$\sigma_{r_n} = p \tag{17}$$

Therefore, by integrating Equation 2 and combining it with Equation 17, it can be obtained that,

$$\sigma_r = p\frac{r_n}{r} \tag{18}$$

By Substituting it into Equation 16, the following equation is available

$$\frac{\partial u}{\partial r} = -\frac{pr_n}{r^2} - \frac{d\sigma'}{de}\frac{\partial e}{\partial r} = -\frac{pr_n}{r^2} + \frac{\sigma_0' \times \ln 10}{C_c} 10^{(e_0-e)/C_c} \frac{\partial e}{\partial r} \tag{19}$$

Therefore, the governing equation can be derived as Equation 20,

$$\frac{1}{r\gamma_w}\frac{\partial}{\partial r}\left(rk_r\left(-\frac{pr_n}{r^2} - \frac{d\sigma'}{de}\frac{\partial e}{\partial r}\right)\right) = \frac{1}{1+e_0}\frac{\partial e}{\partial t} \tag{20}$$

where $\frac{d\sigma'}{de} = -\frac{\sigma_0' \times \ln 10}{C_c} 10^{(e_0-e)/C_c}$

3.3.4 Initial conditions and the boundary conditions

Initially, the increment of effective stress is 0, so the initial void ratio is still homogeneous as Equation 21 shows,

$$e|_{t=0} = e_0 \tag{21}$$

Combined with the previous model description, in this model, the inner boundary and the outer boundary are permeable boundary, the excess pore water pressure is 0. Therefore, the effective stress has the following expression as Equation 22 shows,

$$\begin{aligned} \sigma'|_{r=r_n} &= \sigma_0' + p \\ \sigma'|_{r=r_w} &= \sigma_0' + p\frac{r_n}{r_w} \end{aligned} \tag{22}$$

Correspondingly, the void ratio at the boundary has the following expression as Equation 23 shows,

$$\begin{cases} e|_{r=r_n} = e_0 - C_c \log\left((\sigma_0' + p)/\sigma_0'\right) \\ e|_{r=r_w} = e_0 - C_c \log\left(\left(\sigma_0' + p\frac{r_n}{r_w}\right)/\sigma_0'\right) \end{cases} \tag{23}$$

3.3.5 Calculation of consolidation and deformation

Based on the above controlling equation and boundary conditions, the development of consolidation and deformation over time can be calculated to provide reference for the parameter determination in the preparation of hollow mud column.

According to the effective stress principle, the pore pressure has the following expression as Equation 24 shows,

$$u = \sigma_0' + p\frac{r_n}{r} - \sigma_0' 10^{(e_0-e)/C_c} \tag{24}$$

The average pore water pressure consolidation degree can be expressed as Equation 25,

$$U_p = 1 - \frac{\int_0^H \int_{r_n}^{r_w} 2\pi r u dr dz}{\int_0^H \int_{r_n}^{r_w} (pr_n/r) 2\pi r dr dz} = 1 - \frac{\int_0^H \int_{r_n}^{r_w} r u dr dz}{\int_0^H \int_{r_n}^{r_w} pr_n dr dz} \tag{25}$$

The total deformation has the following form as Equation 26 shows,

$$\Delta V = \int_0^H \int_{r_n}^{r_w} 2\pi r (e_0 - e)/(1+e_0) dr dz \tag{26}$$

It is known that the amount of deformation at any time and the inner radius are related as Equation 27,

$$\Delta V = \int_0^H \int_{r_n}^{r_w} 2\pi r (e_0 - e)/(1+e_0) dr dz = (r^2 - r_n^2)\pi H \tag{27}$$

Then the radius changes over time can be expressed as Equation 28,

$$r = \sqrt{\frac{\int_0^H \int_{r_n}^{r_w} 2\pi r (e_0 - e)/(1+e_0) dr dz}{\pi H} + r_n^2} \tag{28}$$

The relationship between the final radius and the external loading can be expressed as Equation 29,

$$r_f = \sqrt{\frac{\int_0^H \int_{r_n}^{r_w} 2\pi r (e_0 - e_f)/(1+e_0) dr dz}{\pi H} + r_n^2} \tag{29}$$

where $e_f = e_0 - C_c \log_{10}\left(\left(\sigma_0' + p\frac{r_n}{r}\right)/\sigma_0'\right)$.

4 Parametric analysis

4.1 Solution method

Nonlinearity of the governing equation and the consolidation model is mainly considered by the compressibility and permeability variation through the consolidation process. when the consolidation is proceeding, the void ratio decreases, and the compressibility and permeability would be reduced accordingly. To fully consider the nonlinearity of compression and permeability characteristics in the equation, this paper adopts the finite element method to solve the problem, which is carried out in the finite element solving software Flexpde, and the mesh division for this problem is shown in Figure 3. In the finite element model, the compressibility and permeability coefficient is updated in every time step according to the void ratio calculated by the last step, so more accurate results can be obtained.

4.2 Verification of the solution

Considering there is seldom existed consolidation solution for the model in this work, here one-dimensional consolidation with double pervious boundary is applied for the verification. In the verification, the inner radius is assumed close to the outer radius to make the model similar to one-dimensional situation. Meanwhile,

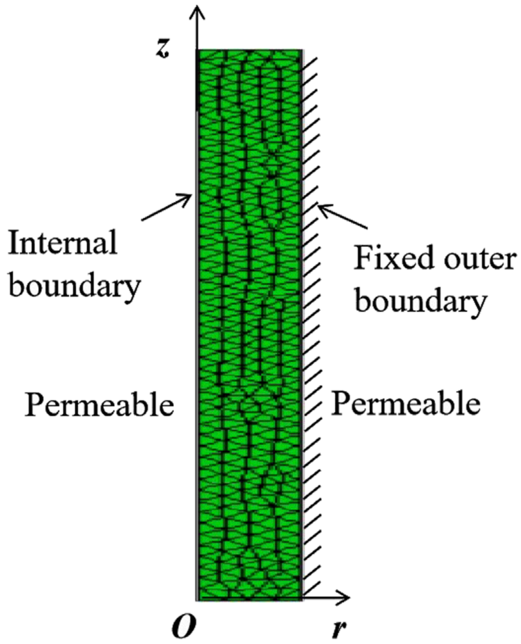

FIGURE 3
Finite element mesh division.

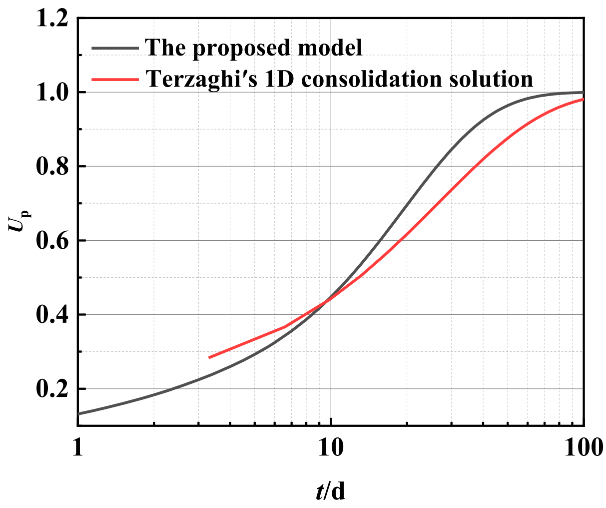

FIGURE 4
Comparison between the reduced solution and existed solution.

nonlinearity is tried to be ignored by assuming the value of C_c/C_k to be 1. The consolidation coefficient used in Terzaghi's solution is calculated by the average permeable coefficient and compression coefficient. The comparison results are shown in Figure 4 below. It can be seen that the reduced solution of this work fits well with Terzaghi's solution. Therefore, the proposed solution in this work is reliable. To be mentioned, because the average consolidation coefficient used in Terzaghi's solution is first larger then smaller than that used in the nonlinear solution, the consolidation degree of the Terzaghi's solution is first larger and then smaller than the proposed solution.

4.3 Parametric analysis

To explore the initial hollow inner diameter, fixed outer diameter, compression index value, external load size and the initial water content of the consolidation process development and the influence of deformation, the reasonable range of different values, and calculated into the control equation, specific calculation of selected parameters as shown in the table below:

4.3.1 Analysis of the influence of initial water content

The initial water content factor is one of the control factors in the soil pile compression molding process, and its initial water content can be controlled by adjusting the mud sampled on-site. According to the nonlinear compression and permeability characteristics of the calculation model in this paper, it is known that the initial values of compressibility and permeability of mud with different initial water contents are also different. Therefore, in the analysis example of the influence of initial water content, the corresponding initial void ratio is calculated based on different initial water contents. Subsequently, the initial void ratio is substituted into the compression curve and the permeability curve to calculate the corresponding initial effective stress and permeability coefficient values. Finally, different initial void ratios, initial permeability coefficients, and initial effective stresses are substituted into the model control equations to calculate their consolidation processes. Figure 5 shows the consolidation degree versus time curves under different initial water contents. From the figure, it can be seen that the development of consolidation degree for all water contents follows a pattern of initially fast, and slow then. The higher the initial water content, the shorter time required for the entire consolidation to be completed. Figure 6 shows the average pore pressure dissipation curves under different initial water contents. From the figure, it can be seen that, similar to the change in consolidation degree, the rate of pore pressure dissipation is relatively faster in cases with higher initial water content. At the same compression time, the effective stress increment corresponding to the larger initial water content is higher. Figure 7 shows the development of the inner diameter over time under different initial water contents. The deformation being influenced by both the initial water content and the change in pore pressure. Because the consolidation speed in the three cases are close to each other, the variation of inner radius is mainly determined by the initial water content. The initial water content with the highest value corresponds to the largest increment in the change of the inner diameter.

4.3.2 The effect of initial inner radius

From the analysis of the modeling part, it is known that the size of the inner diameter in reality affects the distribution of initial excess pore pressure, which in turn affects the consolidation process. Furthermore, revealing the relationship between the initial and final inner diameters has an important impact on the design of process parameters for controlling the size of hollow soil piles. In this section, under the premise of a fixed outer diameter, pressure, and

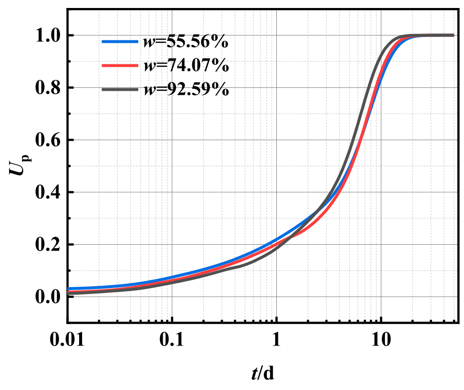

FIGURE 5
Development of consolidation degree for cases with different initial water content.

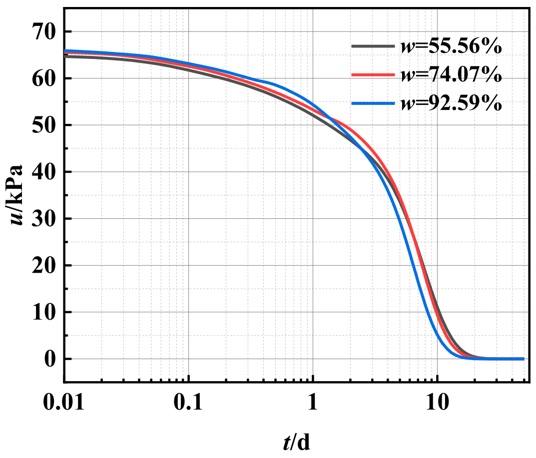

FIGURE 6
Pore water pressure dissipation for cases with different initial water content.

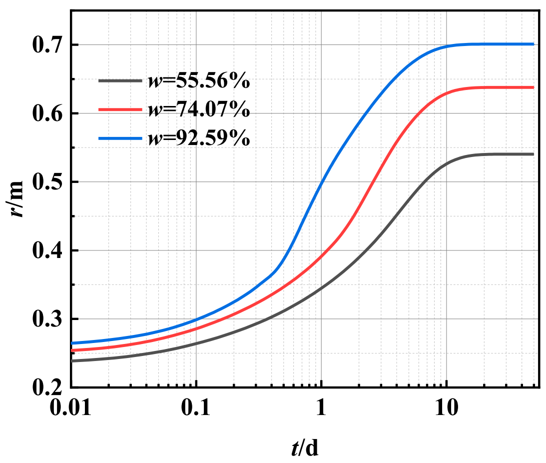

FIGURE 7
Variation of inner radius for cases with different initial water content.

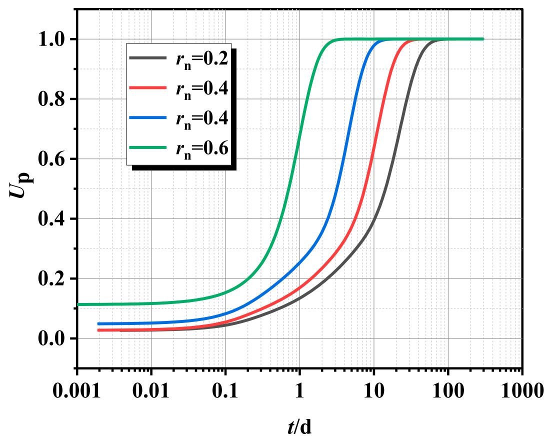

FIGURE 8
Development of consolidation degree for cases with different inner radius.

initial water content, the consolidation behavior under the influence of different initial inner diameters was explored.

Figure 8 shows the development and change curve of consolidation degree under different initial inner diameters. From the figure, it can be seen that the smaller the initial inner diameter, the faster the consolidation speed. This phenomenon is mainly due to the fact that with a fixed outer diameter, the larger the inner diameter of the mud column, the shorter the corresponding path for the discharge of pore water in the soil. Figure 9 shows the average dissipation of excess pore water pressure under different inner diameters. From the figure, it can be seen that the initial average excess pore pressure value corresponding to the larger initial inner diameter of the soil pile is also greater. At the same time, due to the influence of consolidation speed, a crossover phenomenon occurs during the dissipation of pore pressure. In the initial stage, the average excess pore pressure value is also greater in the example with a larger inner diameter. As consolidation progresses, the excess pore pressure value in the example with a larger initial inner diameter dissipates faster, leading to the value gradually becoming less than that in the example with a smaller inner diameter. Figure 10 shows the change in inner diameter over time during the consolidation process under different initial inner diameters. From the figure, it can be seen that the final inner diameter value corresponding to the larger initial inner diameter condition is also greater, but the corresponding increase in inner diameter is smaller, and the growth rate of the inner diameter is slower, similar to the change in consolidation degree.

4.3.3 The effect of outer diameter on the consolidation process

Preparing hollow soil piles by central compaction involves another key geometric parameter, the outer diameter, which is the focus of this section's study. In this part of the calculation, other parameters are kept constant, with specific values shown in Table 1. Figure 11 shows the variation of pore pressure consolidation over time for different outer diameters. From the figure, it can be seen that consolidation is slower with a larger outer diameter,

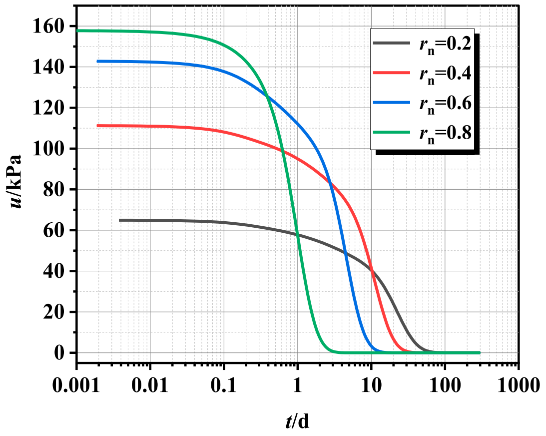

FIGURE 9
Pore water pressure dissipation for cases with different inner radius.

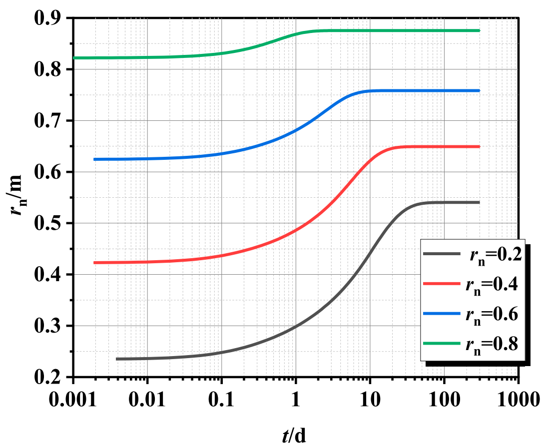

FIGURE 10
Variation of inner radius for cases with different initial inner radius.

and as the outer diameter increases, the linear difference in outer diameter becomes smaller, corresponding to the pattern observed when the inner diameter changes. Figure 12 shows the average excess pore pressure variation for different outer diameters. From the figure, it can be seen that with a constant inner diameter, a smaller outer diameter corresponds to a larger average excess pore pressure. However, because the consolidation speed is faster with a smaller outer diameter, the dissipation rate of the average excess pore pressure is also faster. Therefore, during the dissipation of excess pore pressure, the results shown in Figure 12 indicate that with a smaller outer diameter, the excess pore pressure is initially greater than that of the larger outer diameter cases, but later becomes less than that of the larger outer diameter cases. Figure 13 shows the calculation results for the increase in inner diameter under different outer diameters. From the calculation results, it can be seen that with a larger outer diameter, the deformation of the inner diameter is also greater, but the rate of increase in the inner diameter is similar in the early stages for different outer diameters.

TABLE 1 Basic calculation parameters used for the calculation case analysis.

Parameters	w_0	e_0	σ'_0	C_c	r_n	r_w	p
Values	55.5%	1.5	3.17	0.5	0.2	1	200

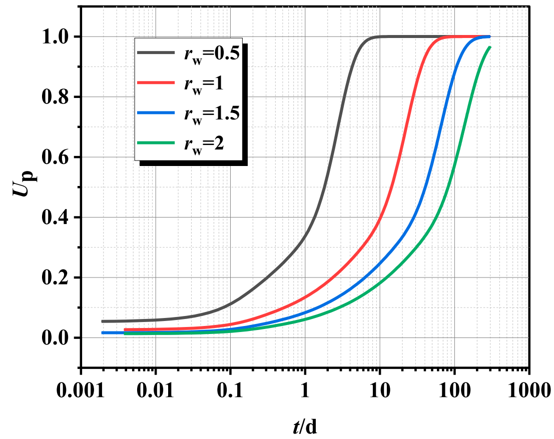

FIGURE 11
Development of consolidation degree for cases with different outer radius.

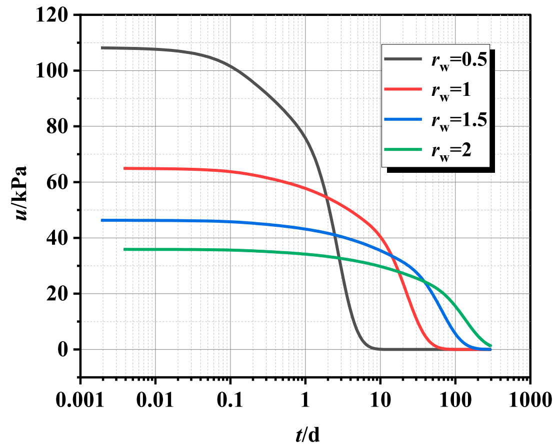

FIGURE 12
Pore water pressure dissipation for cases with different outer radius.

4.3.4 The effect of the magnitude of external loads

The size of the external load is an important factor influencing the final outcome and is also a significant controllable technical parameter in the process of hollow cylinder compression precasting. Therefore, this section investigates the impact of varying external load sizes. In the calculations, apart from the size of the external load, all other factors are consistent with those in Table 1. Figure 14 shows the variation of pore pressure consolidation with time under different external loads. From the figure, it can be seen that, compared with the aforementioned three factors, the impact of

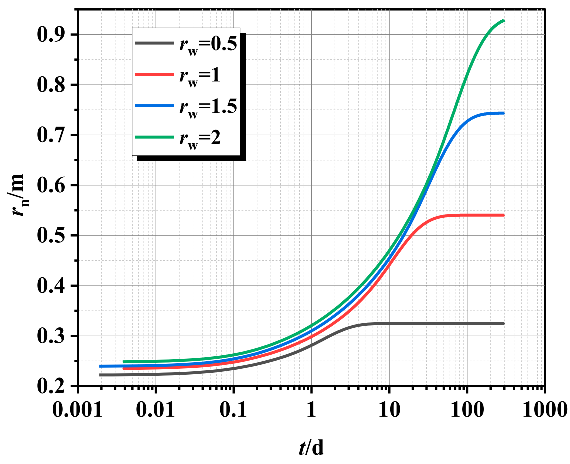

FIGURE 13
Variation of inner radius for cases with different fixed outer radius.

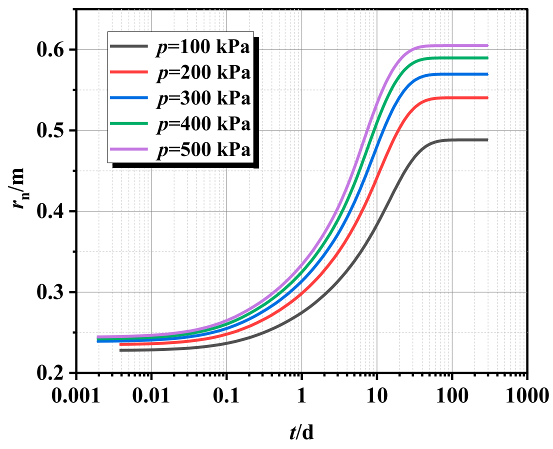

FIGURE 16
Variation of inner radius for cases with different preloading.

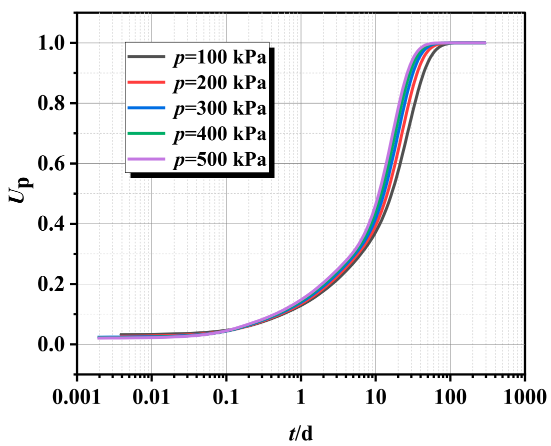

FIGURE 14
Development of consolidation degree for cases with different preloading.

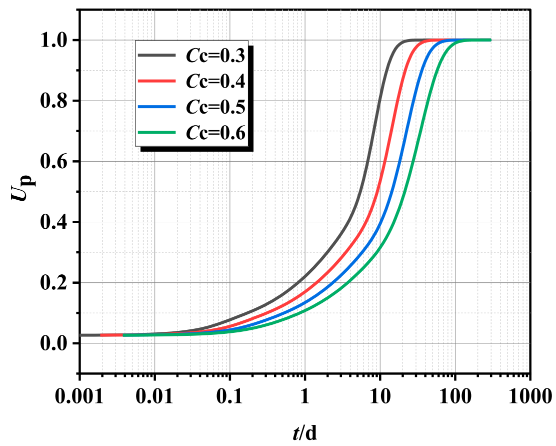

FIGURE 17
Development of consolidation degree for cases with compression index.

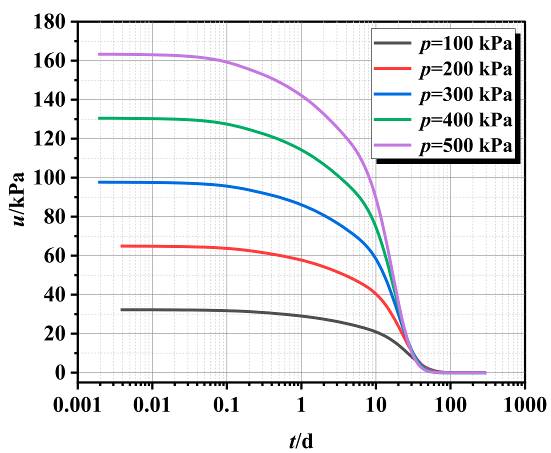

FIGURE 15
Pore water pressure dissipation for cases with different preloading.

external load size on the change in consolidation is not significant. The development of pore pressure consolidation under different external loads is basically the same, with the consolidation development under lower pressure being slightly slower than that under higher pressure. In the classical consolidation solution, there is a conclusion that external load does not affect the development of consolidation, but this is not the case in reality, as shown in Figure 14, where the differences under different loads are mainly due to the effect of the load on the growth process of effective stress, which in turn affects its compressibility and permeability, thus affecting the development of consolidation. Figure 15 shows the average dissipation of excess pore pressure under different loads. From the figure, it can be seen that the larger the external load, the greater the dissipation of the excess pore pressure value. Figure 16 shows the change in internal diameter under different external loads. It can be seen that the larger the external load, the larger the final internal diameter, which means that controlling the size of different external loads can control the shape of the final formed hollow mud

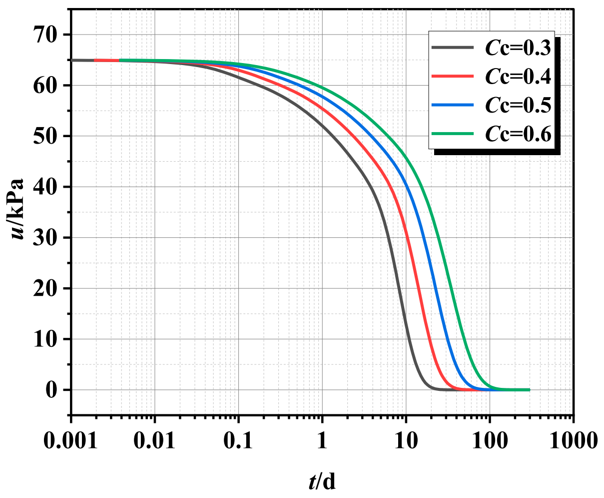

FIGURE 18
Pore water pressure dissipation for cases with compression index.

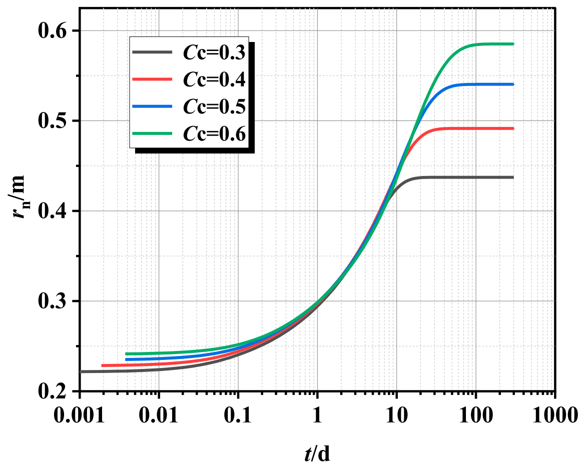

FIGURE 19
Variation of inner radius for cases with different compression index.

column. Considering that the initial void ratio and water content are consistent, different internal diameter sizes imply differences in the final water content. Therefore, in practical applications, to ensure that the prepared hollow soil piles meet strength requirements, it is necessary to comprehensively consider their strength and shape.

4.3.5 The effect of the compression index

Compression index is an important index to measure the compressibility, which can reflect the influence of soil itself characteristics on the consolidation process and consolidation results. This section studies the effect of the compression index on consolidation without determining other parameters including the percolation index. Development curves of pore pressure consolidation under different compression indices are shown in Figure 17. It can be seen from the figure, when the compression index of soil is small, the development speed of consolidation is fast in the whole process, so it can be seen that the consolidation coefficient is relatively large in the corresponding situation. The hyperstatic pore water pressure dissipation curves corresponding to the different compression indices are shown in Figure 18. As can be seen from the figure, because the compression index factor does not affect the average pore water pressure distribution, the dissipation law of pore pressure is basically consistent with the change of pore pressure consolidation. In the case where a small compression index is corresponding, the pore water pressure dissipates faster. Figure 19 shows the curve of time change of internal diameter under different compression exponents, because the size of average pore water pressure dissipation during consolidation is basically the same, but the difference in compressibility will lead to different deformation. As can be seen from the figure, when the compression index is small and the compressibility is poor, the inner diameter changes less, and the final inner diameter formed is also smaller.

5 Conclusion

Based on the axisymmetric model, through the reasonable assumption of load and boundary conditions, establish the annular soil pile considering radial loading and deformation, and analyze the influence of annular soil pile consolidation, which can provide reference for the process parameters of annular soil pile preparation. The specific conclusions are drawn as follows:

(1) The main differences between the middle pressurized consolidation model and the traditional vertical drainage consolidation problem are the radial stress state, deformation state and initial pore water pressure distribution. Based on these assumptions, the governing equation for the consolidation of the soil piles can be derived.
(2) The consolidation speed of soil pile is related to the initial water content, inner and outer diameter, and loading pressure. When the initial water content is higher, the inner diameter is larger, the smaller the outer diameter is smaller, the greater the external load is larger, and the smaller the compression index is, the faster the consolidation speed is, and the shorter the time required to complete the consolidation will be.
(3) The effect of different initial water content factors and the compression index on the dissipation of the mean super-pore water pressure is consistent with the influence of the consolidation development process. Because the influence of the inner and outer diameter factors on the dissipation of the excess pore water pressure is not only in the initial size of the excess pore water pressure, but also in the consolidation velocity, so the dissipation curve of the excess pore water pressure is crossed.
(4) The deformation of hollow soil pile is mainly reflected in the change of its internal diameter. The calculation results show that when the initial water content is larger, the initial internal diameter is smaller, the initial outer diameter is larger, the larger the external load is larger and the compression index is larger, the inner diameter of the consolidation process changes larger.

Data availability statement

The original contributions presented in the study are included in the article/supplementary material, further inquiries can be directed to the corresponding author.

Author contributions

CH Project administration, Writing–original draft, Writing–review and editing. ZF: Methodology, Writing–original draft. SL: Conceptualization, Writing–review and editing. XB: Visualization, Writing–original draft. PY: Software, Writing–original draft. WW: Software, Writing–original draft. XM: Formal Analysis, Writing–original draft. YL: Methodology, Writing–original draft. ZL: Validation, Writing–original draft. BB: Formal Analysis, Writing–original draft.

Funding

The author(s) declare that financial support was received for the research, authorship, and/or publication of this article. This work was funded by the Science and Technology Project of State Grid Jiangsu Electric Power Co., Ltd. (Grant No. J2023004).

Conflict of interest

Authors CH, ZF, PY, WW, XM, YL, ZL, and BB were employed by State Grid Jiangsu Electric Power Co., Ltd. Construction Company.

The remaining authors declare that the research was conducted in the absence of any commercial or financial relationships that could be construed as a potential conflict of interest.

Generative AI statement

The author(s) declare that no Generative AI was used in the creation of this manuscript.

Publisher's note

References

Chu, J., Bo, M. W., and Choa, V. (2006). Improvement of ultra-soft soil using prefabricated vertical drains. *Geotext. Geomembranes* 24 (6), 339–348. doi:10.1016/j.geotexmem.2006.04.004

Deng, Y. B., Xie, K. H., Lu, M. M., Tao, H. B., and Liu, G. B. (2013). Consolidation by prefabricated vertical drains considering the time dependent well resistance. *Geotext. Geomembranes* 36, 20–26. doi:10.1016/j.geotexmem.2012.10.003

Geng, X., Indraratna, B., and Rujikiatkamjorn, C. (2012). Analytical solutions for a single vertical drain with vacuum and time-dependent surcharge preloading in membrane and membraneless systems. *Int. J. Geomechanics* 12 (1), 27–42. doi:10.1061/(asce)gm.1943-5622.0000106

Han, C., Xie, H., Bai, B., Zhang, R., and Huang, Y. (2023). Influence of some key parameters on the efficiency of flocculation–solidification–filter press combined method for sustainable treatment of waste mud slurry. *Sustainability* 15 (21), 15658. doi:10.3390/su152115658

Indraratna, B., Rujikiatkamjorn, C., and Sathananthan, I. (2005). Analytical and numerical solutions for a single vertical drain including the effects of vacuum preloading. *Can. Geotechnical J.* 42 (4), 994–1014. doi:10.1139/t05-029

Lekha, K. R., Krishnaswamy, N. R., and Basak, P. (1998). Consolidation of clay by sand drain under time-dependent loading. *J. geotechnical geoenvironmental Eng.* 124 (1), 91–94. doi:10.1061/(asce)1090-0241(1998)124:1(91)

Liu, S., Cai, Y., Sun, H., Geng, X., Shi, L., and Pan, X. (2021). Consolidation considering clogging effect under uneven strain assumption. *Int. J. Geomechanics* 21 (1), 04020239. doi:10.1061/(asce)gm.1943-5622.0001898

Lu, M., Shan, J., and Li, H. (2022). Theoretical investigation of the consolidation for composite ground with profiled sectional composite piles based on the equivalent ring model. *Rock Soil Mech.* 43 (6), 1513–1532. doi:10.16285/j.rsm.2021.1571

Nguyen, B. P., Do, T. H., and Kim, Y. T. (2020). Large-strain analysis of vertical drain-improved soft deposit consolidation considering smear zone, well resistance, and creep effects. *Comput. Geotechnics* 123, 103602. doi:10.1016/j.compgeo.2020.103602

Zhang, C. L., Guan, F. F., and Li, L. (2014). The progress in the reutillzation treatment and disposal of dredged sediments in China. *Environ. Eng.* 32 (12), 95–99.

Zhang, R., Xu, Z., Liu, S., Wu, Q., and Yang, Y. (2022). Method of preparing composite foundation treatment pile segments by modifying abandoned fluidized sludge. *China Pat. CN115635577A. 2022-11-11.*

Zhu, H., Sun, H., Wang, F., Zou, J., and Fan, J. (2012). Preparation of chitosan-based flocculant for high density waste drilling mud solid–liquid separation. *J. Appl. Polym. Sci.* 125 (4), 2646–2651. doi:10.1002/app.36418

Zong, M., Wu, W., and Mei, G. (2019). Analytical solution for one-dimensional rheological consolidation of soil based on continuous drainage boundary. *Eng. Mech.* 36 (9), 79–88.